

## High Strain-Rate Compressive Properties and Constitutive Modeling of Selected Polymers\*

Kenji NAKAI\*\* and Takashi YOKOYAMA\*\*

\*\* Department of Mechanical Engineering, Okayama University of Science  
Okayama 700-0005, Japan  
E-mail: nakai@mech.ous.ac.jp

### Abstract

The present paper is concerned with constitutive modeling of the compressive stress-strain behavior of selected polymers at strain rates from  $10^{-3}$  to  $10^3/s$  using a modified Ramberg-Osgood equation. High strain-rate compressive stress-strain curves within a strain range of nearly 0.08 for four different commercially available extruded polymers are determined on the standard split Hopkinson pressure bar. The low and intermediate strain-rates compressive stress-strain relations are measured in an Instron testing machine. The five parameters for the modified Ramberg-Osgood equation are determined by fitting to the experimental compressive stress-strain data using a least-squares fit. It is shown that the compressive stress-strain behavior at different strain rates up to the maximum stress can successfully be predicted by the modified Ramberg-Osgood equation. The limitations of the modified Ramberg-Osgood models are discussed.

**Key words:** Compressive Stress-Strain Behavior, Constitutive Modeling, Hopkinson Bar, Modified Ramberg-Osgood Equation, Polymer, Strain Rate Sensitivity

### 1. Introduction

Polymeric materials with low mechanical impedance have been extensively used as one of structural materials for aircraft, automotive and electronic components in terms of weight reduction. These components are often subjected to impact loading in service environments. Therefore, it is needed to characterize the high strain-rate mechanical behavior of polymeric materials. To date, the impact compressive<sup>(1)-(4)</sup>, tensile<sup>(5)-(8)</sup> and torsional<sup>(7), (9)</sup> stress-strain properties of several polymers have been determined with the conventional<sup>(10)</sup> or modified split Hopkinson pressure bar (SHPB). The effects of strain rate and temperature on the compressive characteristics of several polymers were examined using a drop-weight apparatus<sup>(11)-(14)</sup>. In order to accurately describe the high strain-rate stress-strain behavior of the polymers, it is required to develop their strain-rate dependent constitutive equations. Many complicated constitutive models such as nonlinear viscoelastic-plastic models<sup>(15)-(17)</sup>, modified Johnson-Cook model<sup>(18)</sup>, modified Zerilli-Armstrong model<sup>(19)</sup> and nonlinear power law model<sup>(20)</sup> were proposed to predict the stress-strain behavior of the polymers over a wide range of strain rates and temperatures. However, it is very difficult to perform simulations of the response of polymeric structures to dynamic loading using these models with a large number of parameters.

The purpose of the present paper is to model the compressive stress-strain behavior of selected polymers at strain rates from  $10^{-3}$  to  $10^3/s$  using a simple strain-rate dependent constitutive equation. Four different commercially available extruded polymers or ABS (Acrylonitrile Butadiene Styrene), HDPE (High Density Polyethylene), PP (Polypropylene)

\*Received 1 Dec., 2011 (No. 11-0749)  
[DOI: 10.1299/jmmp.6.731]

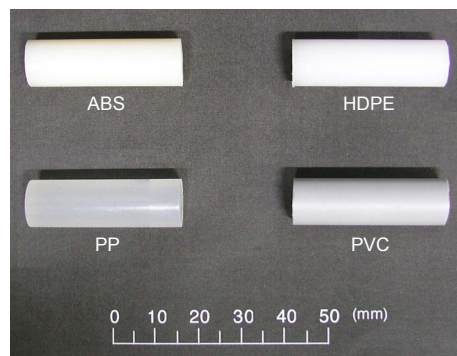
Copyright © 2012 by JSME

and PVC (Polyvinylchloride) were tested at room temperature. Cylindrical specimens with a slenderness ratio  $l/d$  ( $=$  length/diameter) of 0.5 were used in the SHPB tests, and those with  $l/d = 2.0$  were used in the low and intermediate strain-rate tests. The compressive stress-strain loops at strain rates up to about  $10^3/s$  were determined in the conventional SHPB. The compressive stress-strain loops at low and intermediate strain rates were measured with an Instron 5500R testing machine. The strain-rate dependent Ramberg-Osgood equation was applied to model the experimental compressive stress-strain loops over a wide range of strain rates.

## 2. Experimental Procedure

### 2.1 Test Polymers and Specimen Preparation

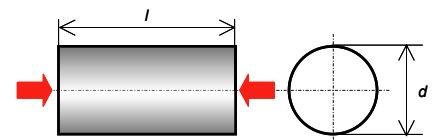
Four different common polymers, i.e., two amorphous polymers: ABS (NAC Group Co., Ltd., Fukui, Japan), PVC (Takiron Co., Ltd., Osaka, Japan) and two semi-crystalline polymers: HDPE (Toyama Keisozai Co., Ltd., Toyama, Japan), PP (NAC Group Co., Ltd., Fukui, Japan) were chosen (see, Fig. 1). Cylindrical specimens were machined out of commercial extruded rods with a diameter of nearly 10 mm into short cylinders with a diameter of 9 mm. The specimen end surfaces were carefully polished with waterproof abrasive paper (#1500). The static specimen's length was determined to be  $l/d = 2.0$  ( $l \approx 18$  mm,  $d = 9$  mm) in accordance with the ASTM Designation E9-89a<sup>(21)</sup> (see, Table 1). The slenderness ratio  $l/d$  of the impact specimen (see, Table 2) was taken as 0.5 ( $l \approx 4.5$  mm,  $d = 9$  mm), falling in an appropriate slenderness ratio range between 0.5 and 1.0 suggested by Gray<sup>(22)</sup> in the conventional SHPB tests. All specimens of the different four polymers were tested in the as-received state.



Abbreviation	Chemical name
ABS	Acrylonitrile-butadiene-styrene
HDPE	High Density Polyethylene
PP	Polypropylene
PVC	Polyvinylchloride

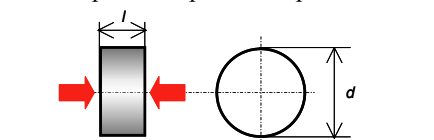
Fig.1 Picture of four different polymers tested

Table 1 Geometry and nominal dimensions of static compression specimen



Polymer	Length $l$ (mm)	Diameter $d$ (mm)	Slenderness ratio $l/d$
ABS	$17.97 \pm 0.03$	8.97	2.0
HDPE	$17.97 \pm 0.02$	8.98	2.0
PP	$17.97 \pm 0.04$	8.96	2.0
PVC	$17.94 \pm 0.04$	8.96	2.0

Table 2 Geometry and nominal dimensions of impact compression specimen



Polymer	Length $l$ (mm)	Diameter $d$ (mm)	Slenderness ratio $l/d$
ABS	$4.44 \pm 0.01$	8.98	0.5
HDPE	$4.43 \pm 0.03$	8.98	0.5
PP	$4.50 \pm 0.07$	8.97	0.5
PVC	$4.44 \pm 0.03$	8.97	0.5

### 2.2 Low and Intermediate Strain-Rate Compression Testing

The low and intermediate strain rate compression tests were conducted on the

cylindrical specimens with  $l/d = 2$  using the Instron 5500R testing machine at crosshead speeds of 1.3 and 130 mm/min, respectively. The specimens were loaded up to a given strain and unloaded at the same crosshead speed. Both ends of the specimen were lubricated with petroleum jelly (white Vaseline) to minimize frictional restraints between the specimen and both loading anvils.

### 2.3 Split Hopkinson Bar Testing

The general arrangement of the SHPB set-up is given in Fig. 2. The SHPB set-up consists of two 2024-T4 Al alloy bars of 2000 mm in length and 10.1 mm in diameter, which remain elastic during the tests. A striker bar made of the same material was 350 mm in length and 10.1 mm in diameter. The mechanical properties of the 2024-T4 Al alloy are as follows: Young's modulus  $E = 73$  GPa; longitudinal elastic wave velocity  $c_o = 5130$  m/s; mechanical impedance  $Z = \rho c_o = 14.2 \times 10^6$  kg/(m<sup>2</sup> s); yield strength  $\sigma_Y = 450$  MPa. The Al alloy bars with low mechanical impedance were used to reduce a drastic impedance mismatch between the polymer specimen [ $Z \approx 1 \sim 2 \times 10^6$  kg/(m<sup>2</sup> s)] and the conventional steel bars [ $Z \approx 40 \times 10^6$  kg/(m<sup>2</sup> s)], which resulted in a transmitted strain signal with a very low signal-to-noise ratio. The specimen was sandwiched between the input and output bars by applying a very small pre-compression load with turning of the head of a support block. As in the static tests, lubricant (or petroleum jelly) was applied to the bar/specimen interfaces to reduce the frictional effects. A pulse shaping technique<sup>(23)</sup> was used to generate well-defined compressive strain pulses without higher frequency components in the input bar. Namely, a 0.2 mm thick 1050 Al disk of nearly 10 mm in diameter was attached onto the impact (left) end of the input bar using a thin layer of petroleum jelly. Details of the test procedure can be found elsewhere<sup>(24)</sup>.

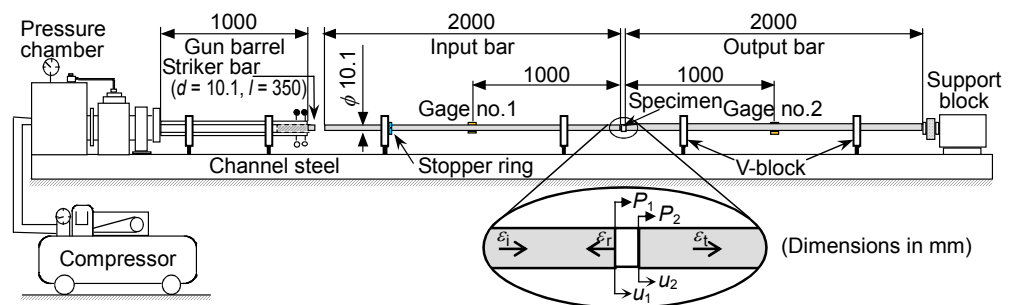


Fig.2 Schematic diagram of conventional split Hopkinson pressure bar set-up (associated recording system not shown)

From the elementary one-dimensional theory of elastic wave propagation, we can determine the nominal strain  $\varepsilon(t)$ , strain rate  $\dot{\varepsilon}(t)$  and stress  $\sigma(t)$  in the specimen from the SHPB test records as<sup>(25)</sup>

$$\varepsilon(t) = \frac{u_1(t) - u_2(t)}{l} = \frac{2c_o}{l} \int_0^t \{ \varepsilon_i(t') - \varepsilon_t(t') \} dt' \quad (1)$$

$$\dot{\varepsilon}(t) = \frac{\dot{u}_1(t) - \dot{u}_2(t)}{l} = \frac{2c_o}{l} \{ \varepsilon_i(t) - \varepsilon_t(t) \} \quad (2)$$

$$\sigma(t) = \frac{P_2(t)}{A_s} = \frac{AE}{A_s} \varepsilon_t(t) \quad (3)$$

Here  $u$  and  $P$  are the displacement and the axial force on both ends of the specimen, respectively, (where subscripts 1 and 2 denote the left and right interfaces, respectively; see the inset in Fig. 2);  $A$ ,  $E$  and  $c_o$  are the cross-sectional area, Young's modulus and the longitudinal elastic wave velocity of the Hopkinson (2024-T4 Al alloy) bars;  $A_s$  is the cross-sectional area of the specimen. Equations (1) to (3) are derived under the assumption

of dynamic force equilibrium across the specimen, which can be expressed as

$$P_1(t) = P_2(t) \quad \text{or} \quad \varepsilon_i(t) + \varepsilon_r(t) = \varepsilon_t(t) \quad (4)$$

where

$$P_1(t) = AE[\varepsilon_i(t) + \varepsilon_r(t)], \quad P_2(t) = AE\varepsilon_t(t)$$

In the above derivations, the incident and reflected strain pulses are time-shifted to the specimen-input bar interface, and the transmitted strain pulse is time-shifted to the specimen-output bar interface. Eliminating time  $t$  through Eqs. (1) to (3) yields the nominal (or engineering) compressive stress-strain and strain rate-strain relations. In this work, the compressive stress and strain are taken as positive.

### 3. Results and Discussion

A number of the SHPB tests were conducted on the four different polymers at room temperature. Figure 3 indicates typical oscilloscope records from the SHPB test on PP. The top trace gives the incident and reflected strain pulses ( $\varepsilon_i$  and  $\varepsilon_r$ ), and the bottom trace gives the strain pulse ( $\varepsilon_t$ ) transmitted through the specimen. The recorded signal data are neither smoothed nor averaged electronically. Note that the duration ( $\approx 340 \mu\text{s}$ ) of the reflected and transmitted strain pulses is much longer than that ( $\approx 210 \mu\text{s}$ ) of the incident strain pulse. This is due to a very long retardation time<sup>(26)</sup> of the polymers. Figure 4 gives the resulting axial stress histories at the front and back ends of the specimen. The nearly overlapping histories clearly indicate that dynamic stress equilibrium is achieved in the specimen over the entire loading duration. Figure 5 presents the resulting dynamic stress-strain loop and strain rate-strain relation in compression. The strain rate does not remain constant during loading as well as unloading, and hence the strain rate  $\dot{\varepsilon} = 650/\text{s}$  given denotes the average one during loading process, which is calculated by dividing the area under the strain rate-strain curve up to the maximum strain ( $\approx 0.08$ ) by the value of its strain. As in the low and intermediate strain rate tests, the dynamic stress-strain loop is not closed, and, consequently, a residual strain of about 0.024 is gradually recovered to zero in time (i.e., *elastic aftereffect*<sup>(27)</sup>). Figure 6 shows the compressive stress-strain loops for PP at three different strain rates. The initial slope (or initial modulus  $E$ ), the flow stress and the area within the loop increase greatly with increasing strain rate. In order to evaluate the effect of strain rate on the compressive properties of the four different polymers, the measured values for the initial modulus (defined as the secant modulus at 0.002 strain) and flow stress at a given strain of 0.05 are plotted in Figs. 7 and 8, respectively, against the average strain rate  $\dot{\varepsilon}$  during loading process. The initial modulus and flow stress increase significantly with increasing strain rate for all polymers. All polymers are found to exhibit inherent dynamic viscoelastic characteristics.

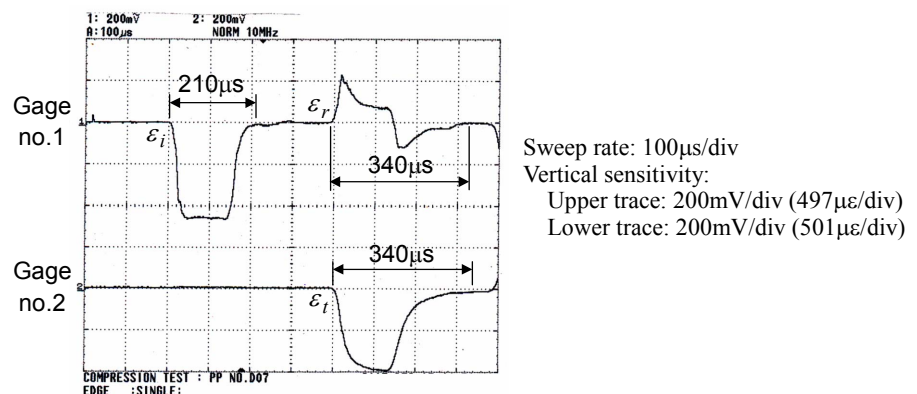


Fig. 3 Oscilloscope traces from SHPB test on PP ( $V_s = 9.6 \text{ m/s}$ )

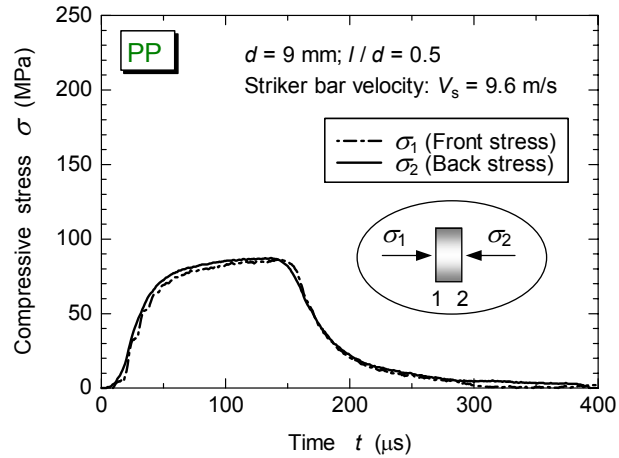


Fig. 4 Time histories of applied stresses on each face of PP specimen

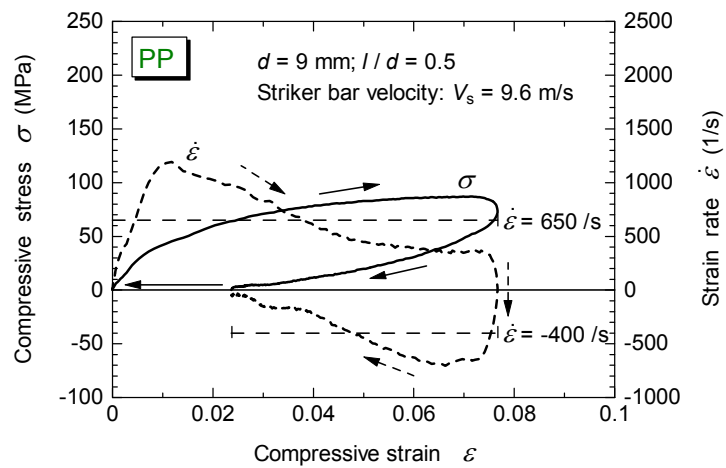


Fig. 5 Dynamic stress-strain loop and strain rate-strain relation for PP in compression

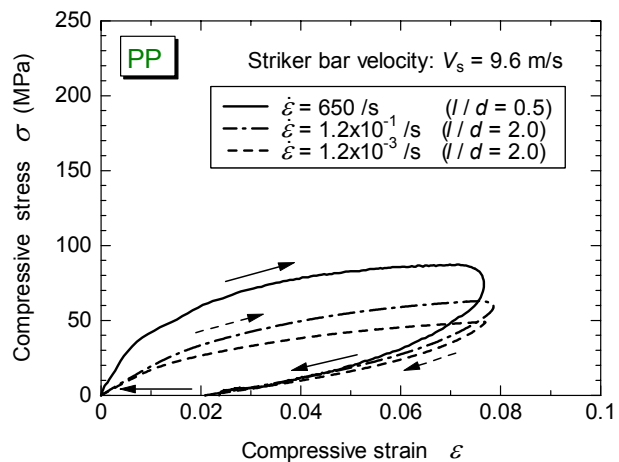


Fig. 6 Compressive stress-strain loops for PP at three different strain rates

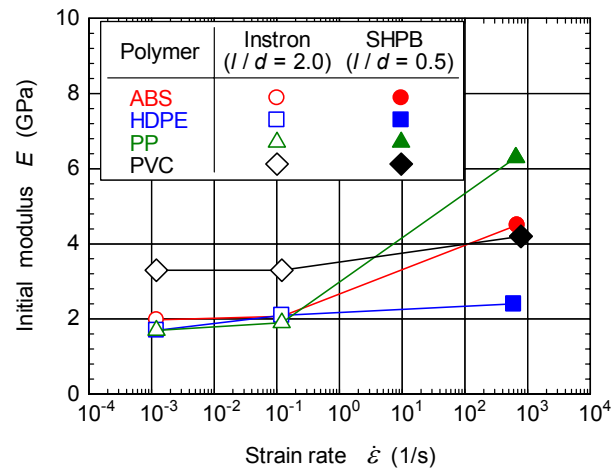


Fig. 7 Effect of strain rate on initial modulus for four different polymers

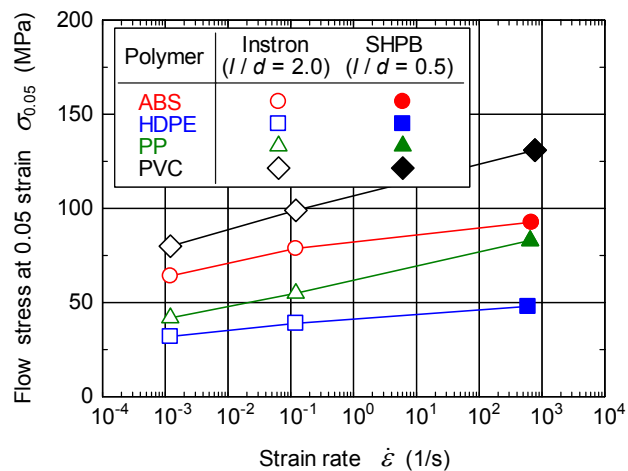


Fig. 8 Effect of strain rate on flow stress at 0.05 strain for four different polymers

In an attempt to quantitatively evaluate the rate dependence of the flow stress at 0.05 strain, two different strain-rate sensitivity parameters  $\beta$  and  $m^{(28)}$  were introduced. The two parameters estimated for all four polymers are summarized in Table 3, where  $\sigma_1$  and  $\sigma_2$  are stresses at the average strain rates  $\dot{\epsilon}_1$  and  $\dot{\epsilon}_2$ , respectively, for a fixed strain of 0.05. The choice of 0.05 strain was made between the common strains at strain rates corresponding approximately to the respective average strain rates during loading. PVC displays the highest strain-rate dependence with respect to  $\beta$ , and PP exhibits the highest strain-rate dependence with respect to  $m$ . A good correlation is observed in the strain-rate sensitivity parameter  $\beta$  between this work and Ref. [4].

Table 3 Strain-rate sensitivity parameters for four different polymers within a range of strain rates from  $\dot{\epsilon}_1 = 1.2 \times 10^{-3}/s$  to  $\dot{\epsilon}_2 = 600/s$

Polymer	$\beta = \frac{\sigma_2 - \sigma_1}{\log(\dot{\epsilon}_2 / \dot{\epsilon}_1)}$ (MPa)	$m = \frac{\log(\sigma_2 / \sigma_1)}{\log(\dot{\epsilon}_2 / \dot{\epsilon}_1)}$ (1/1)
	$\epsilon = 0.05$	$\epsilon = 0.05$
	$\dot{\epsilon}_2 > \dot{\epsilon}_1$	$\dot{\epsilon}_2 > \dot{\epsilon}_1$
ABS	2.12 (2.31)*	0.027
HDPE	1.24 (1.90)	0.031
PP	3.05 (3.91)	0.051
PVC	3.72 (4.84)	0.036

\* Note: values in parentheses are taken from Ref. [4] ( $\epsilon = 0.20$ )

### 4. Constitutive Equations

In an effort to model the compressive stress-strain behavior of the four different polymers, the Ramberg-Osgood equation<sup>(29)</sup> is used, i.e.,

$$\varepsilon(\sigma) = \frac{\sigma}{E} + \left(\frac{\sigma}{H}\right)^{\frac{1}{n}} \quad (5)$$

where  $E$  is the initial (or Young's) modulus,  $H$  the strength coefficient and  $n$  the strain hardening exponent. The first and second terms on the right hand side of Eq. (5) correspond to the elastic strain  $\varepsilon_e$  and the plastic strain  $\varepsilon_p$ , respectively. We can obtain the following relation from Eq.(5):

$$\sigma(\varepsilon_p) = H\varepsilon_p^n = H\left(\varepsilon - \frac{\sigma}{E}\right)^n \quad (6)$$

Taking logarithms of both sides of Eq. (6) gives

$$\log \sigma = \log H + n \log \varepsilon_p \quad (7)$$

Figure 9 shows typical log-log plots of the stress  $\sigma$  - plastic strain  $\varepsilon_p$  data for PP at three different strain rates obtained from Fig. 6. The constants  $H$  and  $n$  were determined by fitting Eq. (7) to the data points on the  $\sigma$  -  $\varepsilon_p$  curves using a least-squares fit. The constant  $H$  corresponds to the value of  $\sigma$  at  $\varepsilon_p = 1$ . The constant  $n$  was determined from the slope of the linear fit line. As can be seen from Fig.9,  $n$  is independent of strain rate up to 650/s, whereas  $H$  depends on the strain rate. Both  $E$  and  $H$  are assumed to be represented by simple power law functions of strain rate  $\dot{\varepsilon}$  as

$$E(\dot{\varepsilon}) = a\dot{\varepsilon}^b; \quad H(\dot{\varepsilon}) = c\dot{\varepsilon}^d \quad (8)$$

where  $a$ ,  $b$ ,  $c$  and  $d$  are material parameters to be determined later. Again taking logarithms of both sides of Eq. (8) leads to

$$\log E = \log a + b \log \dot{\varepsilon}; \quad \log H = \log c + d \log \dot{\varepsilon} \quad (9)$$

Substituting Eq. (8) into Eq. (5), we have the strain-rate dependent Ramberg-Osgood equation (modified Ramberg-Osgood equation)<sup>(30)</sup> as

$$\varepsilon(\sigma, \dot{\varepsilon}) = \frac{\sigma}{a\dot{\varepsilon}^b} + \left(\frac{\sigma}{c\dot{\varepsilon}^d}\right)^{\frac{1}{n}} \quad (10)$$

The measured values for the initial modulus  $E$  and the strength coefficient  $H$  for PP are plotted in Figs. 10 and 11, respectively, against the average strain rate  $\dot{\varepsilon}$  during loading process.

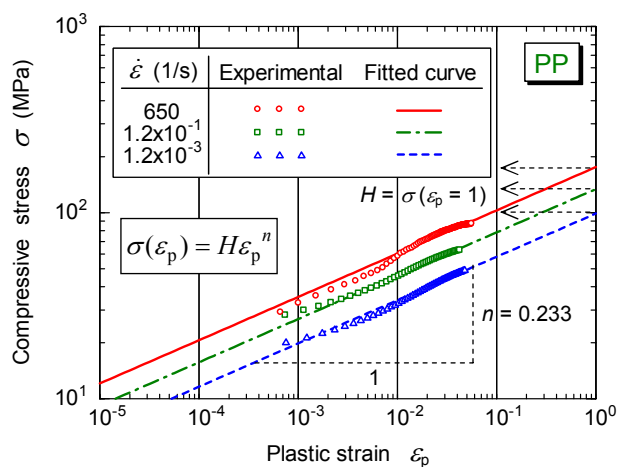


Fig.9 Determination of constants  $H$  and  $n$  in Eq. (6)

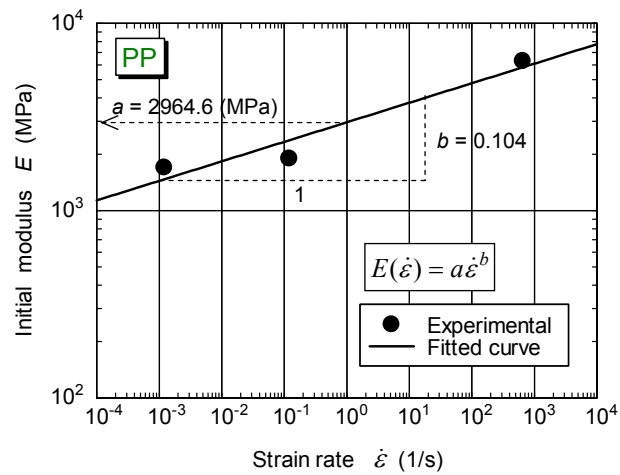


Fig.10 Initial modulus  $E$  as function of strain rate  $\dot{\epsilon}$  for PP. Determination of parameters  $a$  and  $b$  in modified Ramberg-Osgood equation

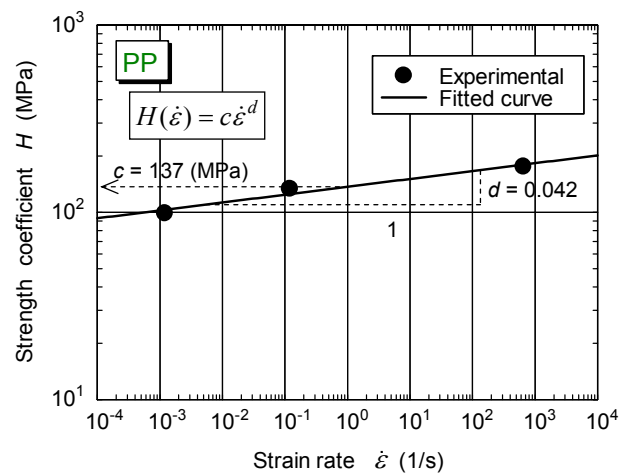


Fig.11 Strength coefficient  $H$  as function of strain rate  $\dot{\epsilon}$  for PP. Determination of parameters  $c$  and  $d$  in modified Ramberg-Osgood equation

Table 4 Parameter values for modified Ramberg-Osgood equation fitted to compressive stress-strain data for four different polymers

Polymer	$a$ (MPa)	$b$ (-)	$c$ (MPa)	$d$ (-)	$n$ (-)
ABS	2779.7	0.066	172.6	0.012	0.2
HDPE	2088.4	0.025	71.6	0.028	0.167
PP	2964.6	0.104	137	0.042	0.233
PVC	3626.8	0.019	185.5	0.031	0.152

The four parameters  $a$ ,  $b$ ,  $c$  and  $d$  were determined by performing the least-squares fit to three sets of measured data points (solid circles) using Eq. (9). The values of parameters in Eq. (10) determined for the four different polymers are listed in Table 4. The fitted curves are shown as the solid lines in Figs. 10 and 11. The parameters  $b$  and  $d$  indicate the strain-rate sensitivity exponents of the initial modulus and flow stress, respectively. A reasonable correlation can be found between the strain-rate sensitivity exponent  $d$  and the strain-rate sensitivity parameter  $m$  given in Table 3. Figure 12 depicts comparisons between

the experimental compressive stress-strain curves and the modified Ramberg-Osgood relations at three different strain rates for the four different polymers. The compressive stress-strain behavior during loading process is accurately predicted by the modified Ramberg-Osgood equations for semi-crystalline polymers (HDPE and PP). In contrast, for the amorphous polymers (ABS and PVC), there are slight discrepancies between measured and predicted compressive stress-strain curves beyond the yield point at low and intermediate strain rates. This is because the amorphous polymers exhibit intrinsic strain-softening phenomena<sup>(17)</sup> after yielding. The strain-softening behavior cannot accurately be described by the modified Ramberg-Osgood equation. Mulliken and Boyce<sup>(17)</sup> predicted successfully the strain-softening behavior after yielding seen in the compressive stress-strain curves at strain rates from  $10^{-4}$  to  $10^4/s$  for the amorphous polymers (PC and PMMA) using nonlinear viscoelastic models. They suggested that it is possible to describe their strain-softening behavior using the nonlinear models with sixteen parameters. Nevertheless, it is very difficult to apply these complicated models to numerical simulations of the mechanical behavior of polymers at various strain rates.

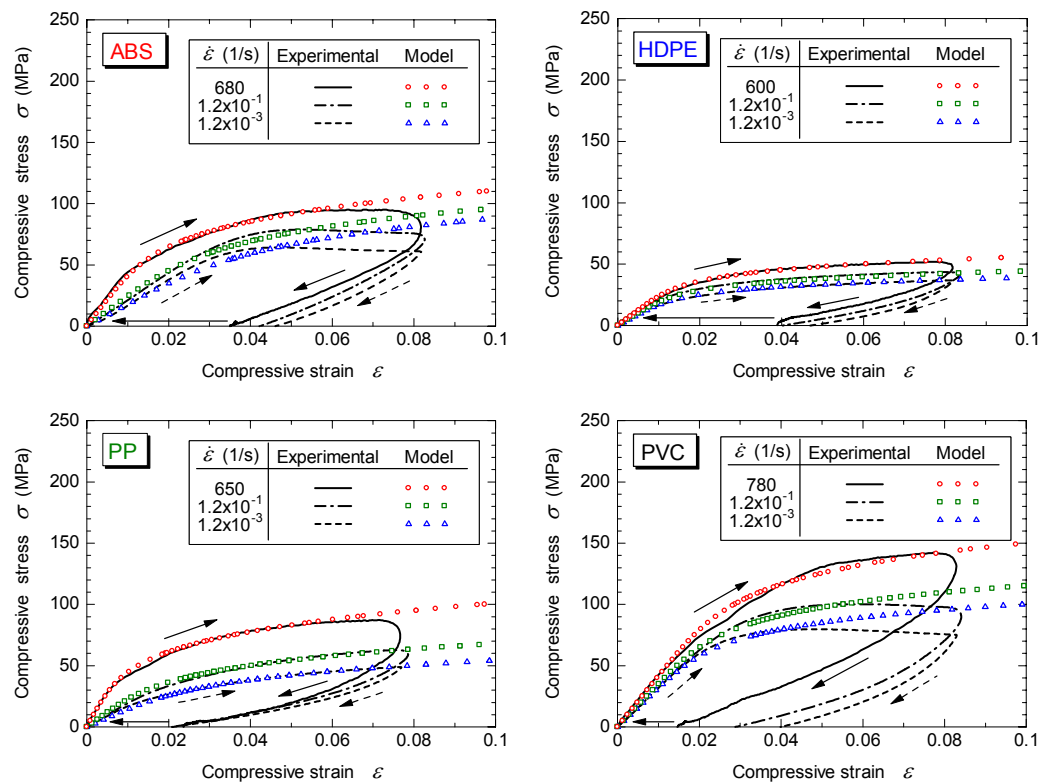


Fig. 12 Comparisons between measured compressive stress-strain curves and modified Ramberg-Osgood relations at three different strain rates for four different polymers

## 5. Conclusions

The strain-rate dependence of the uniaxial compressive stress-strain loops for the four commercial polymers has been investigated with both the standard SHPB and the Instron 5500R testing machine. Constitutive modeling was performed using the modified Ramberg-Osgood equation. From the present study, we can conclude the following:

- (1) All four polymers exhibit intrinsic strain-rate dependent viscoelastic behavior and a high *elastic aftereffect* following complete unloading.
- (2) The initial modulus and flow stress for all four polymers increase greatly with increasing strain rate.

- (3) For the semi-crystalline polymers (HDPE and PP), the compressive stress-strain curves during loading process at strain rates from  $10^{-3}$  to  $10^3/s$  can successfully be predicted by the modified Ramberg-Osgood equations.
- (4) For the amorphous polymers (ABS and PVC), the modified Ramberg-Osgood equation cannot accurately capture the strain softening phenomena after yielding at low and intermediate strain rates.
- (5) The modified Ramberg-Osgood equation cannot be applied to model the unloading stress-strain behavior at low or high strain rates.

### References

- (1) Davies, E.D.H. and Hunter, S.C., The Dynamic Compression Testing of Solids by the Method of the Split Hopkinson Pressure Bar, *Journal of the Mechanics and Physics of Solids*, Vol.11, No.3 (1963), pp.155-179.
- (2) Chiu, S.S. and Neubert, V.H., Difference Method for Wave Analysis of the Split Hopkinson Pressure Bar with a Viscoelastic Specimen, *Journal of the Mechanics and Physics of Solids*, Vol.15, No.3 (1967), pp.177-193.
- (3) Billington, E.W. and Brissenden, C., Mechanical Properties of Various Polymeric Solids Tested in Compression, *International Journal of Mechanical Sciences*, Vol.13, No.6 (1971), pp.531-545.
- (4) Walley, S.M. and Field, J.E., Strain Rate Sensitivity of Polymers in Compression from Low to High Rates, *DYMAT Journal*, Vol.1, No.3 (1994), pp.211-227.
- (5) Shim, V.P.W., Yuan, J. and Lee, S.-H., A Technique for Rapid Two-Stage Dynamic Tensile Loading of Polymers, *Experimental Mechanics*, Vol.41, No.1 (2001), pp.122-127.
- (6) Chen, W., Lu, F. and Cheng, M., Tension and Compression Tests of Two Polymers under Quasi-Static and Dynamic Loading, *Polymer Testing*, Vol.21, No.2 (2002), pp.113-121.
- (7) Gilat, A., Goldberg, R.K. and Roberts, G.D., Strain Rate Sensitivity of Epoxy Resin in Tensile and Shear Loading, *American Society of Civil Engineers, Journal of Aerospace Engineering*, Vol.20, No.2 (2007), pp.75-89.
- (8) Fu, S., Wang, Y. and Wang, Y., Tension Testing of Polycarbonate at High Strain Rates, *Polymer Testing*, Vol.28, No.7 (2009), pp.724-729.
- (9) Fleck, N.A., Stronge, W.J. and Liu, J.H., High Strain-Rate Shear Response of Polycarbonate and Polymethyl Methacrylate, *Proceedings of the Royal Society of London, Series A*, Vol.A429, No.1877 (1990), pp.459-479.
- (10) Kolsky, H., An Investigation of the Mechanical Properties of Materials at Very High Rates of Loading, *Proceedings of the Physical Society*, Vol.B62 (1949), pp.676-700.
- (11) Tardif, H.P. and Marquis, H., Some Dynamic Properties of Plastics, *Canadian Aeronautics and Space Journal*, Vol.9 (1963), pp.205-213.
- (12) Briscoe, B.J. and Hutchings, I.M., Impact Yielding of High Density Polyethylene, *Polymer*, Vol.17, No.12 (1976), pp.1099-1102.
- (13) Hamdan, S. and Swallowe, G.M., The Strain-Rate and Temperature Dependence of the Mechanical Properties of Polyetherketone and Polyetheretherketone, *Journal of Materials Science*, Vol.31, No.6 (1996), pp.1415-1423.
- (14) Roland, C.M., Twigg, J.N., Vu, Y. and Mott, P.H., High Strain Rate Mechanical Behavior of Polyurea, *Polymer*, Vol.48, No.2 (2007), pp.574-578.
- (15) Chase, K.W. and Goldsmith, W., Mechanical and Optical Characterization of an Anelastic Polymer at Large Strain Rates and Large Strains, *Experimental Mechanics*, Vol.14, No.1 (1974), pp.10-18.
- (16) Sadd, M.H. and Morris, D.H., Rate-Dependent Stress-Strain Behavior of Polymeric Materials, *Journal of Applied Polymer Science*, Vol.20, No.2 (1976), pp.421-433.
- (17) Mulliken, A.D. and Boyce, M.C., Mechanics of the Rate-Dependent Elastic-Plastic

- Deformation of Glassy Polymers from Low to High Strain Rates, *International Journal of Solids and Structures*, Vol.43, No.5 (2006), pp.1331-1356.
- (18) Chen, W. and Zhou, B., Constitutive Behavior of Epon 828/T-403 at Various Strain Rates, *Mechanics of Time-Dependent Materials*, Vol.2, No.2 (1998), pp.103-111.
- (19) Jordan, J.L., Siviour, C.R., Foley, J.R. and Brown, E.N., Compressive Properties of Extruded Polytetrafluoroethylene, *Polymer*, Vol.48, No.14 (2007), pp.4184-4195.
- (20) Naik, N.K., Shankar, P.J., Kavala, V.R., Ravikumar, G., Pothnis, J.R. and Arya, H., High Strain Rate Mechanical Behavior of Epoxy under Compressive Loading: Experimental and Modeling Studies, *Materials Science and Engineering A*, Vol. 528, No.3 (2011), pp.846-854.
- (21) ASTM E9-89a, *Annual Book of ASTM Standards*, Vol.03.01, (1995), pp.98-105, American Society for Testing and Materials, Philadelphia.
- (22) Gray, G.T. III, Classic Split-Hopkinson Pressure Bar Testing, *ASM Handbook, Vol.8, Mechanical Testing and Evaluation*, (2000), pp.462-476, ASM International, Materials Park, OH.
- (23) Song, B. and Chen, W., Loading and Unloading Split Hopkinson Pressure Bar Pulse-Shaping Techniques for Dynamic Hysteretic Loops, *Experimental Mechanics*, Vol.44, No.6 (2004), pp.622-627.
- (24) Nakai, K. and Yokoyama, T., Strain Rate Dependence of Compressive Stress-Strain Loops of Several Polymers, *The Japan Society of Mechanical Engineers, Journal of Solid Mechanics and Materials Engineering*, Vol.2, No.4 (2008), pp.557-566.
- (25) Lindholm, U.S., Some Experiments with the Split Hopkinson Pressure Bar, *Journal of the Mechanics and Physics of Solids*, Vol.12, No.5 (1964), pp.317-335.
- (26) Ward, I.M. and Sweeney, J., *An Introduction to the Mechanical Properties of Solid Polymers*, 2nd Edition, (2004), p.57, John Wiley & Sons, Ltd, Chichester.
- (27) Dieter, G.E., *Mechanical Metallurgy*, SI Metric Edition, (1988), p.434, McGraw-Hill, London.
- (28) Malatyński, M. and Klepaczko, J., Experimental Investigation of Plastic Properties of Lead over a Wide Range of Strain Rates, *International Journal of Mechanical Sciences*, Vol.22, No.3 (1980), pp.173-183.
- (29) Ramberg, W. and Osgood, W.R., Description of Stress-Strain Curves by Three Parameters, *Technical Note, No.902, National Advisory Committee for Aeronautics*, Washington DC (1943).
- (30) McLellan, D.L., Constitutive Equations for Mechanical Properties of Structural Materials, *AIAA Journal*, Vol.5, No.3 (1967), pp.446-450.